Heliyon 8 (2022) e12339

Contents lists available at ScienceDirect

Heliyon

journal homepage: www.cell.com/heliyon

Research article

Antihypertensive activity of roasted cashew nut in mixed petroleum fractions-induced hypertension: An *in vivo* and *in silico* approaches

Jacob Kehinde Akintunde [a], Victoria Omoyemi Akomolafe [a,b,*], Odunayo Anthonia Taiwo [a,b], Iqrar Ahmad [c,d], Harun Patel [d], Adeola Osifeso [a], Adefuye Oluwafemi Olusegun [a], Oluwafemi Adeleke Ojo [e,*]

[a] *Applied Biochemistry and Molecular Toxicology Research Group, Department of Biochemistry, College of Biosciences, Federal University of Agriculture Abeokuta Nigeria*
[b] *Department of Biochemistry, College of Natural and Applied Sciences, Chrisland University, Ajebo Abeokuta, Ogun-state*
[c] *Department of Pharmaceutical Chemistry, Prof. Ravindra Nikam College of Pharmacy, Gondur, Dhule, 424002, Maharashtra, India*
[d] *Division of Computer Aided Drug Design, Department of Pharmaceutical Chemistry, R. C. Patel Institute of Pharmaceutical Education and Research, Shirpur, 425405, Maharashtra, India*
[e] *Phytomedicine, Molecular Toxicology, and Computational Biochemistry Research Lab, Department of Biochemistry, Bowen University, Iwo, 232101, Osun State, Nigeria*

ARTICLE INFO

Keywords:
Angiotensin converting enzyme
Systolic blood pressure
Petroleum fractions
Cashew nuts
Computational tools

ABSTRACT

Consumption of water polluted by crude oil is a major environmental problem typical in exploration areas. Numerous health complications such as high blood pressure, myocardial infarction, and other heart complications are prevalent and ravaging. These have gradually become age-defiling disease conditions that are usually maintained with lifestyle changes and diet control. The effect of dietary supplementation with 10% and 20% roasted cashew nuts (RCN) on systolic blood pressure and angiotensin converting enzyme I (ACE I) activities in mixed petroleum fraction (MPF) induced toxicity was studied in male Wistar rats through the modulation of the renin-angiotensin system. The phytochemicals in RCN were quantified using the high performance liquid chromatography (HPLC) technique. To predict likely binding affinity and stability, computational methods such as molecular docking, ADME, and molecular dynamic simulation were used. Out of the seven phytochemicals identified, rutin, gallic acid, and quercetin had the greatest quantities. Similarly, rutin had the highest binding affinities with ACE I, -10.7 kcal/mol, followed by quercetin, at -9.1 kcal/mol. During the molecular dynamics simulation, all of the identified phytochemicals demonstrated good pharmacokinetic capabilities and remained stable at their respective binding sites. Subsequent *in vivo* validation studies revealed that RCN was able to attenuate the effect of MPF by significantly ($p < 0.05$) lowering the systolic blood pressure and ACE I activity in comparison to the reference medication, atenolol. We recommend that cashew nuts be explored as dietary snacks as well as a low-cost, easily available component of supplements for the treatment of high blood pressure.

1. Introduction

Many environmental contaminants and their constant levels of pollution are hazardous in nature. They contribute immensely to damage to human, animal, and plant health. Even at low concentrations, several pollutants and their metabolic products can be carcinogenic, mutagenic, and immunotoxic [1]. Because of their hydrophobicity and low volatility, crude oil exploration and distribution are well-established water contaminants in the environment, posing a threat to both aquatic and terrestrial organisms. Oral ingestion of crude oil or its products, or drinking contaminated water, is a route for possible toxicants to enter the human system [2]. Toxicants in the environment, such as petroleum compounds, can induce neurologic and cardiovascular problems, as well as drain the brain [3].

The zinc metalloprotein angiotensin-converting enzyme (ACE), also known as dipeptidyl carboxypeptidase I or kininase II, is a key component of the renin–angiotensin system (RAS). It regulates blood pressure by converting angiotensin I into angiotensin II, a strong vasoconstrictor that binds to its receptor and other vasoactive peptides to exert its pressor actions in tissues and cells [4]. The reduction of ACE activity leads to a decrease in angiotensin II production and bradykinin metabolism, resulting in a systematic dilatation of the arteries and veins. Inhibition of

* Corresponding authors.
E-mail addresses: vicyem4real@gmail.com (V.O. Akomolafe), oluwafemiadeleke08@gmail.com (O.A. Ojo).

https://doi.org/10.1016/j.heliyon.2022.e12339
Received 11 April 2022; Received in revised form 5 May 2022; Accepted 6 December 2022

the RAS was found to be useful in reducing renal dysfunction, cardiovascular diseases (CVD) and Alzheimer's disease associated with increased blood pressure in animal models [5].

Nuts stand out among plant foods because of their unusual nutrient content, which includes complex carbohydrates and unsaturated fats, largely in the form of monounsaturated fatty acids (MUFA; predominantly oleic acid) and polyunsaturated fatty acids (PUFA) [6]. Nuts' wide range of nutrients, as well as synergy between them and with other dietary components, are likely to explain their beneficial effects [6].

A cashew nut is a kidney-shaped drupe of the *Anacardium* family and a true fruit commonly eaten in a roasted form. It is packed with energy, antioxidants, minerals, vitamins, and phytochemicals that are essential for robust health. It has been reported to enhance protection from diseases and cancers, and prevention of coronary artery diseases and stroke by lowering LDL-cholesterol due to the high MUFA content [7]. Mustapha and others (2015) confirmed the role of cashew nuts in enhancing protein, fat, and carbohydrate metabolism and serving as a booster for the immune system. This they attributed to the level of vitamins, pantothenic acid (Vit.B_5) and zinc mineral. Cashew tree parts (leaves, roots, and nuts) have been used in folk medicine for several treatments of diseases with a limited scientific basis of their action.

Computational tools have become particularly useful in drug discovery and design to speed up the process while still maintaining efficiency and efficacy [8]. Hence, this study seeks to establish the phytochemical content of cashew nuts and determine, via computational analysis, their interaction with ACE as a possible therapeutic mechanism in vasoconstriction. Also, validation of the outcome with notable biochemical vasoconstriction indicators.

2. Methodology

2.1. Preparation of roasted cashew nut powder

The protocol described by Omosuli et al. [9] was used to make roasted cashew nut (RCN) powder. Healthy cashew nuts were collected from a farm in Abeokuta, Ogun State, Nigeria. The botanical identification and authentication were done with a voucher number UAHA0021/8/001 by the Department of Forestry and Wildlife Management, College of Environmental Resources Management, Federal University of Agriculture, Abeokuta, Ogun State, Nigeria. Two kilograms of cashew nuts were cleaned to remove impurities, then soaked in water to prevent scorching during the roasting process by placing the nuts in a plastic container filled with water in a 60:40 ratio of water to nut for 10 min, and the water was drained out. To remove the nuts from the shells, the cashew samples were broken with a manual cashew kernel cutter and dried in the oven at 40 °C for 5 h. The seeds were roasted for 24 h in a Cabolite DHG 9053A oven by Zenith Lab (Jincheng industrial area, Jintan, Jiangsu, China) at a controlled temperature of 60 °C. To achieve cream-colored nuts, the roasted seed covering testa was removed and winnowed. The roasted cashew nut seeds were blended into a fine powder using a food processor (HR 2811 Philip Model). The grounded samples were kept in an airtight sample container in a refrigerator (4 °C) for further analysis.

2.2. Quantification of compounds by HPLC

High performance liquid chromatographic analysis was carried out with a PDA detector connected to a system processor with standard certification for analysis on 12 mg/ml ethanolic extract of roasted nuts powder from *Anacardium occidantale*. The HPLC was run at 200nm–500nm wavelength using a reverse phase of C_{18} column with a flow rate of 1 ml/min maintained using the binary mode of the gradient system. Different combinations of the solvents (1:4, 4:1, 1:3, 1:1) of methanol and water were used, with the optimum peak at 1:1. To identify the compounds, standards of flavonoids (catechenol, naringenin, quercetin, apigenin, rutin, kaempferol, catechin) and phenolic acids (p-hydrobenzoic acid, p-coumaric acid, gallic acid, ferrulic acid, caffeic acid) obtained from Sigma Aldrish Chemical Co (St. Louis, MO, USA) were used. The peaks were identified by comparing their retention time (RT) and absorption spectrum to that of the standard compounds. All chromatographic operations were carried out at ambient temperature and in triplicate.

2.3. Target and ligand preparation and docking

The 3D structure of angiotensin-converting enzyme (ACE) was downloaded from the Protein Data Bank (PDB with ID number 2C6N), while the ligand structures were downloaded from Pubchem. Protein minimization was done using Chimera 1.14 before uploading to Pyrx for docking with the ligands.

2.4. Molecular dynamics simulation study

Molecular dynamic (MD) simulations were used to analyze the dynamics and stability of phyto-compounds in complex with human Angiotensin-I converting (2C6N) protein [10, 11]. The study was carried out on the phyto-compounds showing the best results among the studied phyto-compounds. Firstly, the protein preparation wizard with an OPLS3e force field was used to prepare, optimize, and minimize the docked complexes produced by Autodock [12, 13, 14]. The "system builder" panel of Desmond was used to generate a solvent system with a single point charge (SPC) water model with an orthorhombic water box. The protein-ligand complexes were neutralized with counter ions (Na^+ and Cl^-) and a 0.15 M NaCl salt concentration was built to mimic physiological conditions using the ionization module of the System Builder [15, 16]. Using Desmond's default protocol, the prepared systems were relaxed and energy was minimized. The energy-minimized protein ligand system was subjected to MD simulations using the NPT (isothermal–isobaric) ensemble, with the temperature kept at 310 K by a Nose-Hoover chain thermostat and the pressure kept at 1 bar by a Martyn-Tobias-*Klein barostat* [17, 18, 19]. The simulation was carried out for a period of 100 ns, and simulation trajectories were retrieved at every 100 ps interval. A total of 1000 trajectories were assessed using a simulation interaction diagram for analyzing the ligand protein RMSD value and predicting the binding orientation of the ligand. With the help of the *thermal_mmgbsa.py* script of the Prime/Desmond module, the entire trajectories of each system were considered to estimate the binding free energy through the MM-GBSA (Molecular Mechanics-Generalized Born Surface Area) method. Details of the MM-GBSA procedure can be found in our previous publications [20, 21, 22].

2.5. ADMET/toxicity determination

Swissadme was used to determine the ADME and toxicity properties of the phytochemicals.

3. Biochemical analysis

3.1. Chemicals

The substrate Hippuryl-histidyl-leucine, as well as Tris-HCl buffer, ethyl acetate, copper sulphate pentahydrate, sodium tartrate, sodium hydroxide, potassium iodide, and bovine serum albumin were obtained from Sigma Chemical Co (St. Louis, MO, USA). All the other chemicals used in this experiment were of the highest purity, while the water was glass distilled.

3.2. Sample collection

The refined petroleum products used: diesel, kerosene, and petrol were obtained from the Nigerian National Petroleum Corporation (NNPC), fuel station in Abeokuta, Ogun State, Nigeria. Mixed petroleum

Table 1. Diet formulation for basal and supplemented diets for control and test groups.

	CONTROL	MFH	MFH + ATN	MFH + RCN_{10}	MFH + RCN_{20}	$RICN_{10}$	RCN_{20}
CORN OIL	10.00	10.00	10.00	10.00	10.00	10.00	10.00
PREMIX	3.00	3.00	3.00	3.00	3.00	3.00	3.00
SUCROSE	2.00	2.00	2.00	2.00	2.00	2.00	2.00
CORN STARCH	63.67	63.67	63.67	57.69	51.67	57.69	51.67
CASEIN	21.33	21.33	21.33	17.31	13.33	17.31	13.33
RCN	-	-	-	10.00	20.00	10.00	20.00
TOTAL	100.00	100.00	100.00	100.00	100.00	100.00	100.00

fractions (MPF) of the refined products were prepared at a ratio of 1:1:1 v/v.

Healthy fresh nuts of *Anacardium occidantale* were obtained from a farm at Abeokuta, Ogun State, Nigeria. The botanical identification and authentication were carried out at the Department of Forestry and Wildlife Management, College of Environmental Resources Management, Federal University of Agriculture, Abeokuta, Ogun State, Nigeria. A voucher number UAHA0021/8/001 was assigned to the sample deposited at the Departmental Herbarium.

3.3. Animals

Eleven weeks old, thirty-five adult male Wistar albino rats weighing between 150 and 170 g were obtained from the Department of Physiology, University of Ibadan, Nigeria, and moved to the animal house, College of Biosciences, Federal University of Agriculture, Abeokuta. The animals were given free access to food and water after being acclimatized.

3.4. Experimental design

Thirty-five rats (n = 5) were randomly allocated into seven groups, each with five animals for a period of twenty-eight days (fourteen days of exposure to the toxicant and fourteen days of treatment). Toxicity was caused by giving 0.2 ml/kg body weight of mixed petroleum fractions (MPH) by oral gavage to all groups except group I, group VI, and group VII. The animals were given the mixture every other day for fourteen (14) days. After receiving the petroleum fractions, the animals were provided a supplemented diet for fourteen days (except control).

Group I (Control): This group was placed on a basal diet and was not given the mixed petroleum fraction.

Group II (MPF): This is the group that is given a basal diet and mixed petroleum fractions.

Group III (MPF + ATN): serve as the control placed on the basal diet, MPH and atenolol (50 mg/kg).

Group IV (MPF +10% RCN): serve as the induced group placed on a diet supplemented with roasted cashew nuts (10%).

Table 2. The phenolic and flavonoid compounds in RCN (n = 3).

Roasted cashew nut compounds	Concentration (mg/mg)
Gallic acid	8.92 ± 0.07
Catechenol	3.23 ± 0.05
p-Coumaric acid	4.17 ± 0.01
Rutin	9.38 ± 0.01
Quercetin	8.63 ± 0.05
Kamferol	2.20 ± 0.05
Naringinin	3.54 ± 0.02

Note: The results are expressed as mean ± SEM of three determination.

Group V (MPF +20% RCN): serve as the induced group placed on a diet supplemented with roasted cashew nuts (20%).

Group VI (10% RCN): serve as the control group placed on a diet supplemented with roasted cashew nuts (10%).

Group VII (20% RCN): serves as the control group placed on a diet supplemented with roasted cashew nuts (20%).

The procedure for this investigation was authorized by the Department of Biochemistry Ethics Committee under the number 17/0261 and followed the requirements for the care and well-being of research animals (NIH, 1985).

3.5. Diet formulation

In the laboratory, fresh *A. occidantale* nuts were roasted, crushed into powder, and sieved through a 2 mm pore size. The diets were developed in collaboration with the Department of Animal Production and Health, Federal University of Agriculture, Abeokuta, using a modified technique of Akintunde et al. [23] (Table 1). The vitamin premix (mg or IU/g) has the following composition; 3200 IU vitamin A, 600 IU vitamin D3, 2.8 mg vitamin E, 0.6 mg vitamin K3, 0.8 mg vitamin B1, 1 mg vitamin B2, 6 mg niacin, 2.2 mg pantothenic acid, 0.8 mg vitamin B6, 0.004 mg vitamin B12, 0.2 mg folic acid, 0.1 mg biotin H2, 70 mg choline chloride, 0.08 mg cobalt, 1.2 mg copper, 0.4 mg iodine, 8.4 mg iron, 16 mg manganese, 0.08 mg selenium, 12.4 mg zinc, 0.5 mg antioxidant.

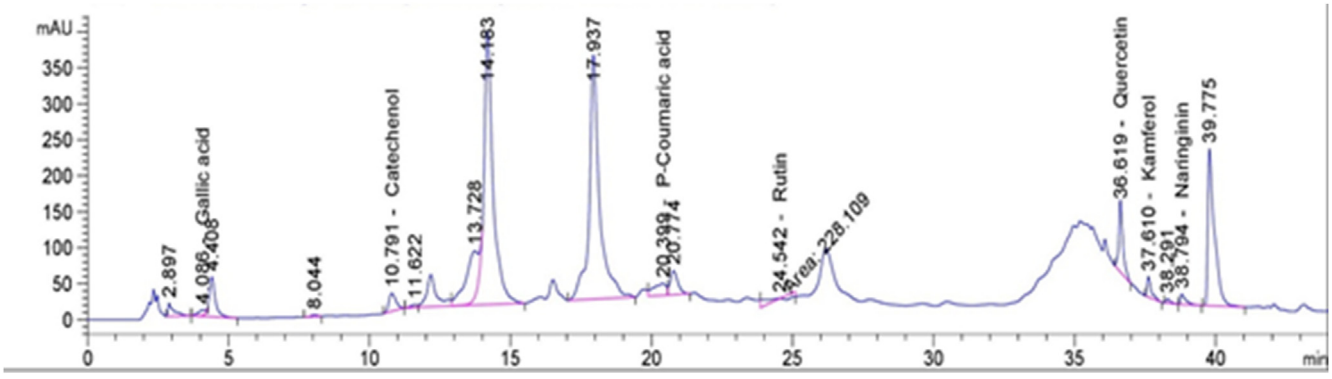

Figure 1. High performance liquid chromatogram showing the phytochemicals with their peak.

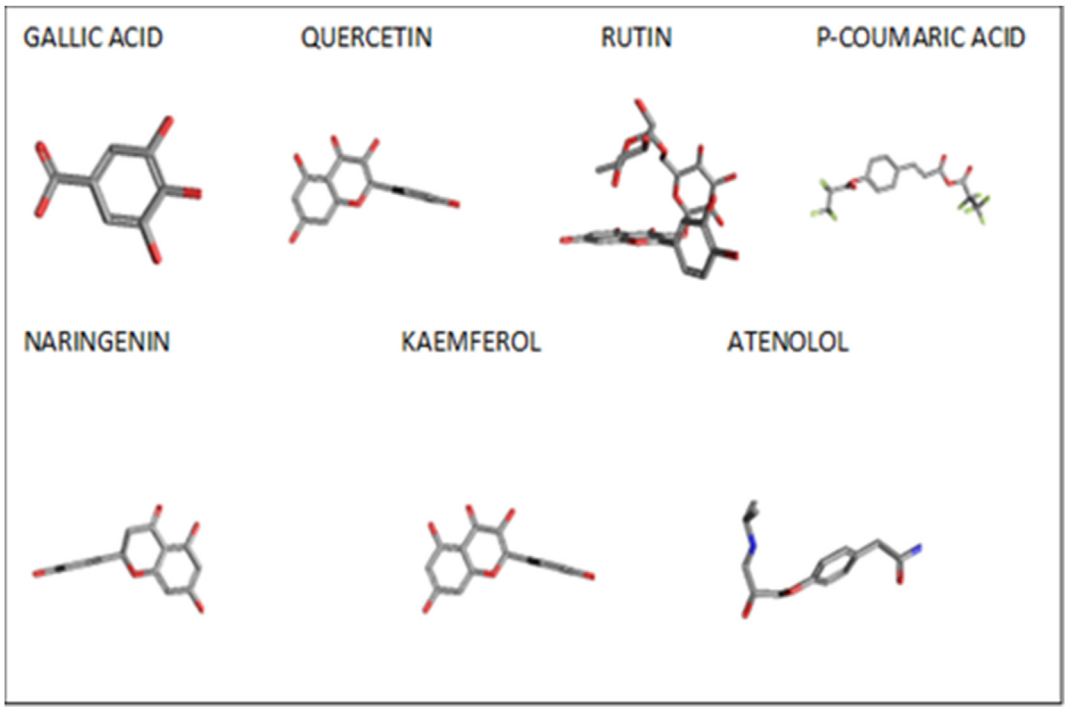

Figure 2. Represents the structure of the compounds docked against ACE I.

Table 3. Binding affinity (kcal/mol) of compounds with ACE I.

	LIGAND	MOLECULAR WEIGHT	DOCKING SCORE
1	GALLIC ACID	170.12	-5.8
2	P-COUMARIC ACID	164.16	-6.2
3	**RUTIN**	610.52	**-10.7**
4	**QUERCETIN**	302.24	**-9.1**
5	KAEMPFEROL	286.24	-8.7
6	NARINGENIN	272.25	-8.6
7	**ATENOLOL**	266.34	-7.2

3.6. Hemodynamic indicator determination

The systolic blood pressure (SBP) was measured in live animals by tail-cuff plethysmography (Kent Scientific; RTBP 2000 Rat Tail Blood System). Rats were conditioned with the apparatus before measurements were taken. Two consecutive systolic blood pressure readings were taken during and after the experiment.

3.7. Blood collection

After the treatment, the animals were subjected to euthanasia having previously been anesthetized with ketamine or xylazine. Blood was collected via cardiac puncture and then transferred to an anticoagulant-free bottle using a hypodermic needle and a 5 mL syringe. The blood sample was allowed to coagulate for 30 min at room temperature. The serum was then separated from the clotted blood by centrifugation.

3.8. Angiotensin converting enzyme activity assay

Angiotensin-l-Converting Enzyme (ACE) activity was determined by the method of Cushman and Cheung [24]. The result was expressed in serum ACE activity per mg of protein.

3.9. Determination of protein concentration

The protein concentration of brain homogenate was determined by the biuret assay method as described by Gornal *et al.* [25] with some modification using serum albumin as a standard.

3.10. Statistical analysis

All data are presented as means ± S.E.M. of the indicated number of experiments. Statistical significance was assessed by one-way analysis of variance followed by Duncan's multiple range test at the significant level of $p < 0.05$, considered to represent a significant difference in all experiments. The statistical analyses were performed using the software package GraphPad Prism 6.

4. Results

4.1. Characterization of the roasted cashew nut extract

Figure 1 shows the HPLC phenolic and flavonoid profiles of RCN extract, which revealed the presence of gallic acid, rutin, naringin, kaempferol, p-coumaric acid, catechol and quercetin with their peaks when compared with phenolic and flavonoid standards, while Table 2 shows the concentration of the components with rutin as the major component.

4.2. Molecular docking

The structures of compounds identified and standard compound are shown in Figure 2. Table 3 shows the binding affinity results of the compounds and ACE I with their respective molecular weights. Rutin has the highest binding affinity (−10.7 kcal/mol), followed by quercetin (9.1 kcal/mol), kaempferol (−8.7 kcal/mol), and naringenin (−8.6 kcal/mol). The standard compound atenolol recorded -7.2 kcal/mol. The 2D

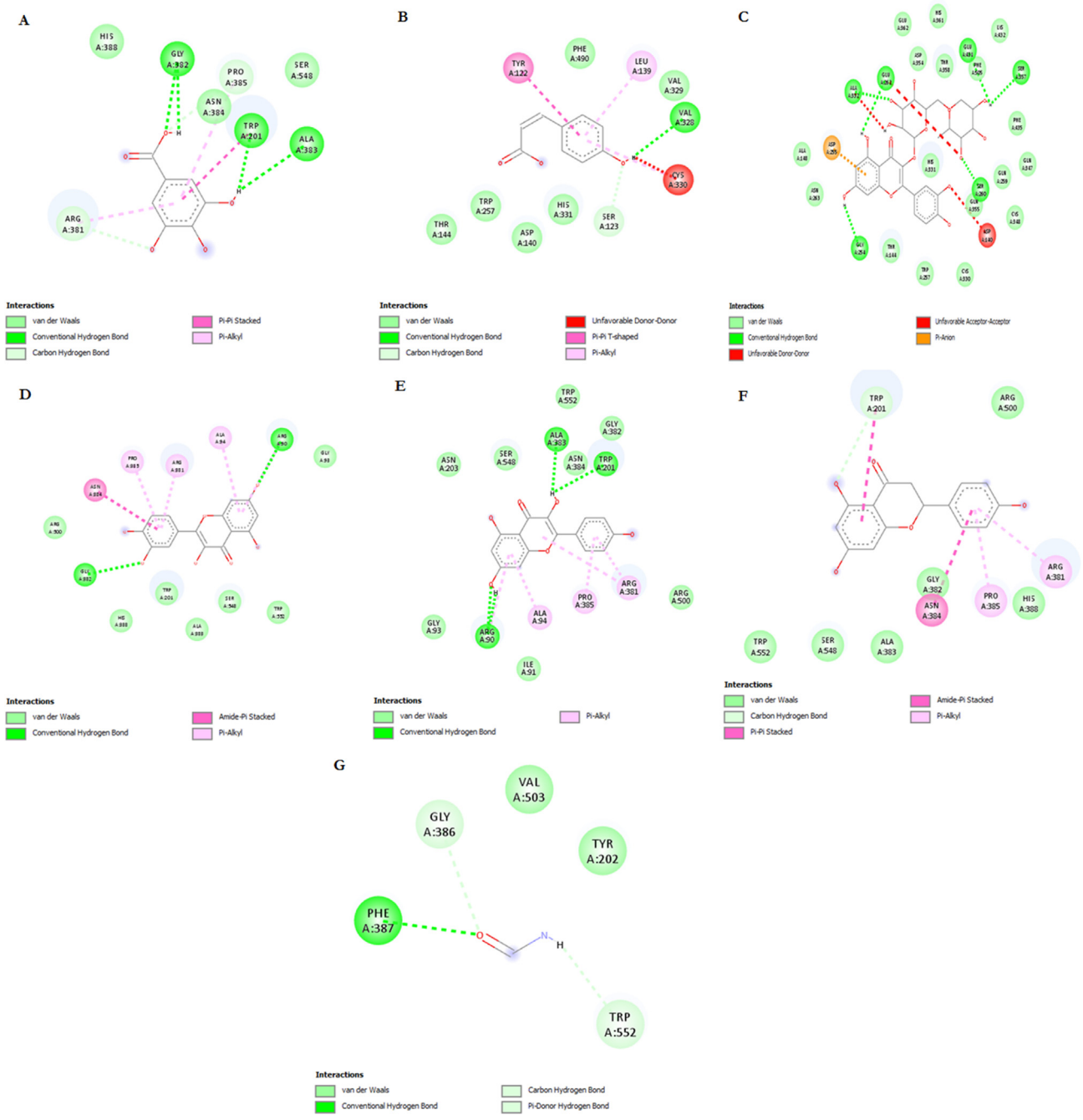

Figure 3. (A–G): 2D structures of the ligands complexed with ACE I protein. (A.: Gallic acid complexed ACE I, B.: p-Coumaric acid complexed ACE I, C.: *Rutin complexed* ACE I, D.: Quercetin complexed ACE I, E.: Kaempferol complexed ACE I, F.: Naringenin complexed ACE I, G.: Atenolol complexed ACE I).

interactions of the compounds and the protein targets is shown in Figure 3 (A-G).

4.3. Pharmacokinetic properties

Table 4 shows the pharmacokinetics and druglikeness properties of the test compounds and standard drug, atenolol. Rutin has a molecular weight of over 610 mg/mol, low GI absorption, and BB permeant. It also violates 3 Lipinski rules. However, quercetin with the next best binding affinity had a molecular weight of 302.24, high GI absorption, and is not BB permeant with no violation of both Lipinski and Verber's rules.

4.4. Molecular dynamics (MD) simulation

A 100 ns MD simulation in an explicit hydration environment was performed to evaluate the stability of phyto-compounds quercetin, rutin, and atenolol as controls in a complex with human Angiotensin-I converting (2C6N) protein. The root mean square deviations (RMSD) of Cα atoms of protein, the RMSD of ligand, the protein root mean square fluctuation (RMSF), and the protein ligand contacts for all complexes were analyzed to determine the stability of the trajectory during MD simulation. The RMDS of each frame derived from the entire trajectory can be used to examine the structural conformation of the protein Cα atom during the MD simulation. The 2D interaction diagram and RMSD

Table 4. Water solubility (Log S), pharmacokinetics, bioavailability, and druglikeness values of test compounds.

	GALLIC ACID	P-COUMARIC ACID	RUTIN	QUERCETIN	KAEMPFEROL	NARINGENIN	ATENOLOL
Rotatable Bond	1	2	6	1	1	1	8
TPSA	97.99	57.53	269.43	131.36	111.13	86.99	84.58
ESOL Log S	-1.64	-2.02	-3.3	-3.16	-3.31	-3.49	-1.3
GIA	High	High	Low	High	High	High	High
BB permeant	No	No	Yes	No	No	No	No
Pgp substrate	No	No	Yes	No	No	Yes	No
CYP2C9 inhibitor	No	No	No	No	No	No	No
Log Kp	-6.84	-6.26	-10.26	-7.05	-6.7	-6.17	-7.81
Lipinski	0	0	3	0	0	0	0
Verber	0	0	1	0	0	0	0
BAV	0.54	0.85	0.17	0.55	0.55	0.55	0.55
Leadlikeness	1	1	1	0	0	0	1
SA	1.22	1.61	6.52	3.23	3.14	3.01	2.51

Legend: TPSA-total polar surface area, GIA-gastrointestinal absorption, BBB- Blood brain barrier, Pgp: P-glycoprotein, BAV- bioavailability, S.A-synthetic accessibility.

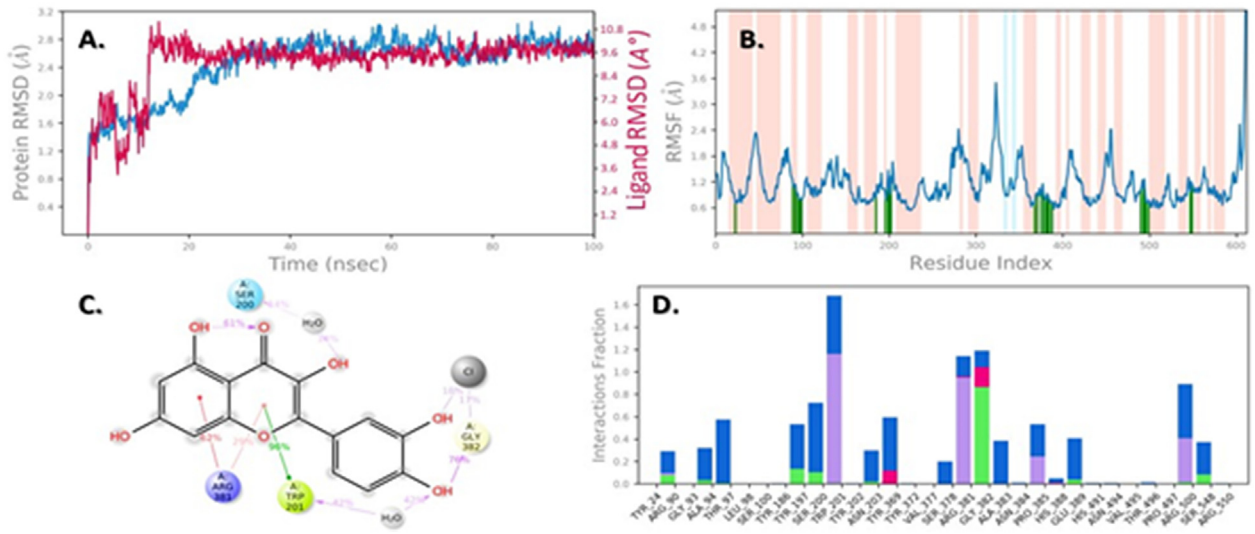

Figure 4. (A-D): 2D interaction diagram, MD stimulation trajectory and RMSD plot for Quercetin ligand-protein complex.

plot for each ligand-protein complex have been presented in Figures 4A, 5A, and 6A. The low deviation and consistent fluctuation of the RMSD throughout the simulation can describe the protein–ligand complex's stability. For each simulated complex, the protein Cα atom RMSD was estimated and found to be very low for all proteins [26, 27]. For the quercetin, rutin, and atenolol complexes, the average value of protein Cα atom RMSD was found to be 2.41 Å, 1.89 Å, and 2.36 Å, respectively. This low average RMSD indicates that all MD simulations have been well-equilibrated. In addition to the RMSD of the protein Cα atom, the RMSD of the ligand was calculated. After an initial period of ligand RMSD fluctuations due to equilibration, quercetin and rutin reached an equilibration state and remained stable throughout the MD simulation. There is no significant RMSD fluctuation in this complex, inferring that the system has attained a more stable state than the initial state. On the other hand, Atenolol displayed extremely stable RMSD throughout the simulation time with the least variance, but a little high RMSD was observed at 45 ns, which later stabilized at 3.0 Å. From the above data, all complexes appeared to be equilibrated with a minor variation, indicating that the systems folded into more stable conditions than the native structure.

4.5. Post simulation: binding free energy analysis

To calculate the binding free energy from the MD simulation trajectory of identified phyto-compounds along with atenolol, the MM-GBSA method was used. Post-simulation MM-GBSA was calculated at every tenth frame from frame 0 to 1000, yielding a total of 100 conformations for each simulated complex (Tables S1, S2, and S3). The protein ligand interactions were also assisted by non-bonded interactions such as van der Waals (vdW), Coulombic interaction, lipophilic, general born solvation energy and covalent interactions to finally converge the complexes after the 100 ns simulation displayed in Table 5. The assessed binding energies for quercetin-2C6N, rutin-2C6N, and atenolol-2C6N were recorded at -43.185, -35.554, and-30.080 as kcal/mol, respectively. A lower value indicates a stronger bond [20, 21, 22]; binding energies decreases were labeled as quercetin-2C6N < rutin-2C6N < atenolol-2C6N. Above all, MD simulation data indicates that quercetin and rutin have more stability and binding affinity than atenolol in the human angiotensin-I converting protein.

4.5.1. Effect of dietary supplementation of roasted cashew nuts on systolic and diastolic blood pressure in MPF-induced toxicity

To ascertain the effect of MPF on blood pressure, oral administration of MPF by gavage was found to cause a significantly higher final systolic blood pressure (SBP) and diastolic blood pressure (DBP) when compared with the animals in the control group, establishing that MPF can induce vasoconstriction. However, it could be observed that dietary supplements from RCN as well as the standard hypertensive effectively caused a significant reduction of SBP and DBP in the hypertensive MPF group (Figures 7 and 8).

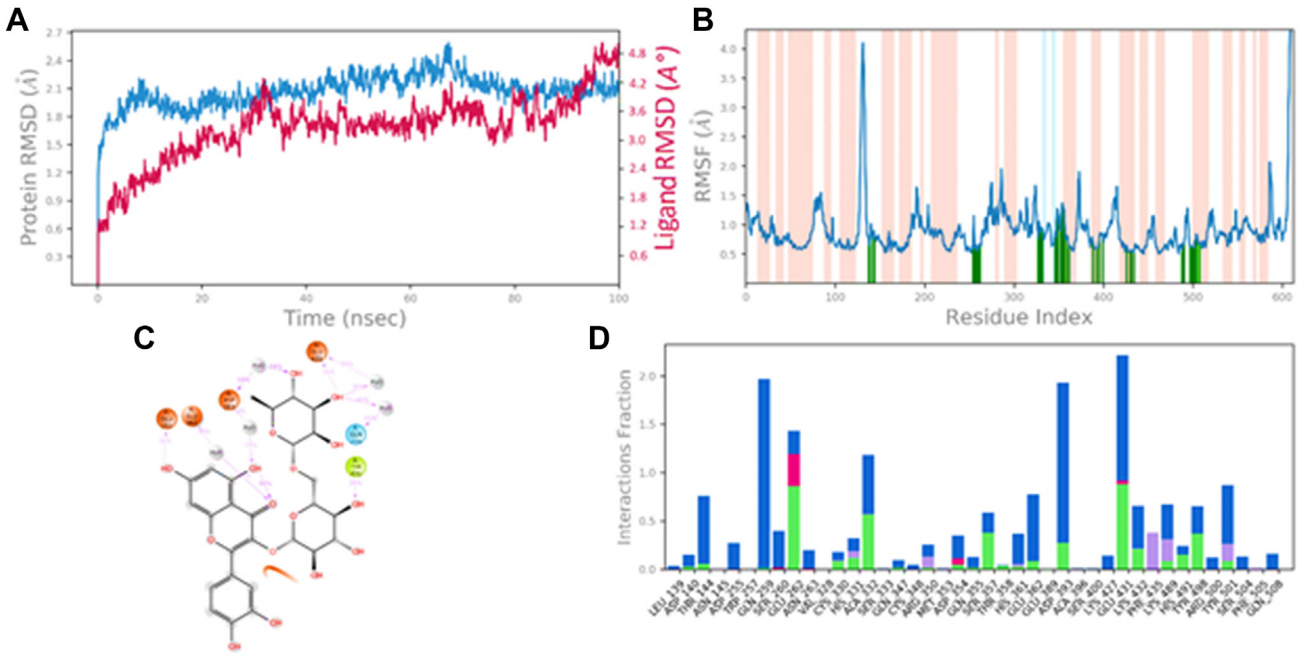

Figure 5. (A-D): 2D interaction diagram, MD stimulation trajectory and RMSD plot for Rutin ligand-protein complex.

4.5.2. Effect of dietary supplementation of roasted cashew nuts on ACE activities in MPF induced toxicity

Serum ACE activity reflects the index implication of hypertension in an animal model. Figure 9 reveals that there was a significant elevation ($p < 0.05$) of ACE activity in animals exposed to MPH when compared with the control. The treatment of rats with a dietary supplement from RCN resulted in a significant ($p < 0.05$) decrease in ACE activity, indicating a restoration of its activities.

5. Discussion

Overactivity of the renin-angiotensin-aldosterone system (RAAS), the kalikerenin kinin system, and the sympathetic nervous system, as well as hereditary influences, may all play a part in the pathophysiology of hypertension. Lifestyle changes, such as maintaining a balanced diet, are among the most common methods of minimizing the risk of hypertension [28]. In this study, HPLC of RCN extract revealed that its components are flavonoids such as rutin, quercetin, kaempferol, and naringenin. Flavonoids have been shown to reduce the risk of cardiovascular disease, cancer, and neurodegenerative diseases, among others [29]. It is also high in phenolics like gallic acid and p-coumaric acid. The majority of the results obtained were comparable to those published by Celina et al. [30], albeit with a few exceptions.

Molecular docking is a prediction tool used to determine the result. It revealed rutin with the highest binding affinity with ACE I, then quercetin, kaempferol, and naringenin, all greater than the affinity of the

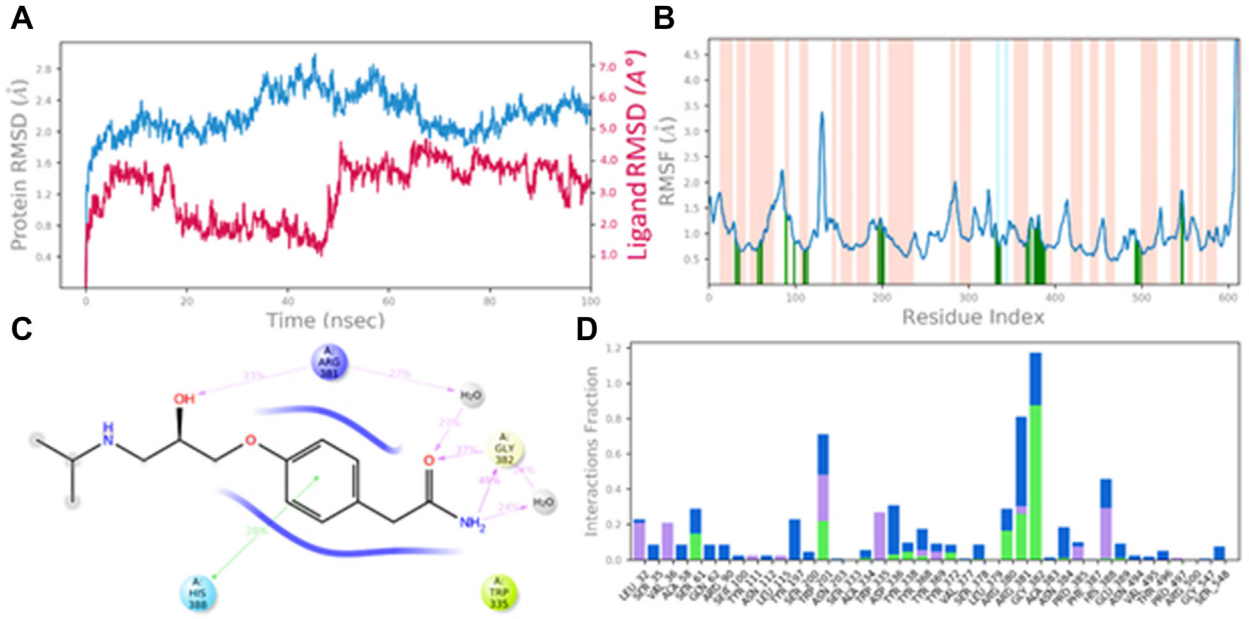

Figure 6. (A-D): 2D interaction diagram, MD stimulation trajectory and RSMD plot for Atenolol ligand-protein complex.

Table 5. MM-GBSA binding free energies components for the protein ligand complexes obtained from molecular dynamics trajectories.

Complex Name	ΔG Bind	ΔG Bind Coulomb	ΔG Bind Covalent	ΔG Bind H bond	ΔG Bind Lipo	ΔG Bind Solv GB	ΔG Bind vdW
Quercetin-2C6N	-43.185	-7.949	1.278	-1.296	-10.123	17.797	-32.552
Rutin-2C6N	-35.554	-31.785	5.063	-4.029	-12.397	59.328	-49.945
Atenolol-2C6N	-30.080	-11.758	2.694	-1.286	-9.420	19.184	-30.080

standard drug atenolol for the protein. However, the molecular weight of rutin and its ability to cross the BB barrier call for caution as a potential drug. It also violates 3 Lipinski rule; Lipinski's rule of five is used to determine a chemical compound's drug-likeness in terms of certain biological or pharmacological properties required of an effective oral drug in humans [31].

To investigate the impact of single amino acids on the stability of any protein–ligand interaction, the RMSF parameter is critical. It's the change in orientation of each amino acid Cα atoms during the simulation compared to the native state's initial orientation [32, 33, 34]. The RMSF of each amino acid was computed using the MD simulation trajectory, as shown in Figure 4B, 5B, and 6B. In the RMSF graphic, loop areas are portrayed by a white band, whereas α-helices and β-sheets are depicted by blue and pink bars, respectively. Although α-helices and β-sheets were stiff, loop areas tended to change the most throughout simulation. The participation of interaction residues between human Angiotensin-I converting protein and phyto-compound is depicted by the vertical green lines on the plot's X-axis. The mean RMSF can be used to assess how the individual amino acids in a protein structure fluctuate. For quercetin, rutin, and atenolol complexes, the average RMSF was revealed to be 1.14 Å, 0.91 Å, and 1.03 Å, respectively. According to the RMSF plot, quercetin, rutin, and atenolol interacted with 32, 41, and 42 amino acids of human angiotensin-I converting protein, respectively. It can be seen that highest fluctuation was observed with Asp 324(3.49 Å), Gly 235 (3.12 Å), Ile 611 (3.75 Å), Asp 612 (6.01 Å) in Quercetin-2C6N complex, Glu 609 (3.70 Å), Asn 131(3.73 Å), Lys 132 (4.10 Å), Gly 610 (4.78 Å), Asp612(5.2 Å) Ile611 (5.25 Å) in Rutin-2C6N complex and Lys132 (3.07 Å), Glu609 (3.08 Å), Ala 134 (3.11 Å), Thr133 (3.38 Å), Asn131 (3.65 Å) Gly610 (5.56 Å), Ile611 (6.39 Å), Asp612 (8.03 Å) in Atenolol-2C6N complex which is not interacted with lead compounds. The RMSF results clearly indicated that the amino acids of human Angiotensin-I converting protein that interacted with phyto-compounds stayed constant throughout the simulation.

The quercetin-2C6N complex's 2D ligand interaction diagram revealed that the 3,5,7-trihydroxy-4H-chromen-4-one scaffold had two strong hydrophobic interactions, π-cation and π-π stacking, with Arg 381 and Trp 201 accounting for 91% and 96.6% of the total simulation trajectory, respectively (Figure 4c). Rutin-2C6N complex, charged negative amino acids (Asp and Glu) mainly interacted with direct hydrogen bonding and amino acid mediated hydrogen bonding. whereas at 36% of the simulation trajectory, residue Tyr498 formed π-π stacking interactions with the hydroxyl group (Figure 5c). At 28% of the simulation time in the control atenolol-2C6N complex, the phenyl ring forms a π-π stacking interaction with the hydrophobic residue His 388. Amino acids Arg381 and Gly 382 interacted with atenolol through bidentate amino acid mediated hydrogen bonding and direct hydrogen bonding, respectively (Figure 6c).

The interaction of each system during the 100 ns simulation was examined to better understand the affinity of identified phyto-compounds with human Angiotensin-I converting protein. During the MD run, the protein-ligand contact histogram clearly shows that the discovered phyto-compounds are stabilized by interacting with the human angiotensin-I converting protein, mostly through hydrophobic, water-bridged, hydrogen-boding, and ionic contacts (Figures 4D, 5D, and 6D).

By converting the precursor angiotensin I into angiotensin II, the peptide responsible for initiating blood pressure-raising processes, angiotensin converting enzyme (ACE) plays a key role in RAAS. As a result, inhibiting ACE is a possible method of controlling RAAS expression. The stimulation of the renin–angiotensin system via enhanced ACE activity was reflected in an increase in systolic blood pressure after oral administration of MPF. The elevated ACE activity in the serum is in

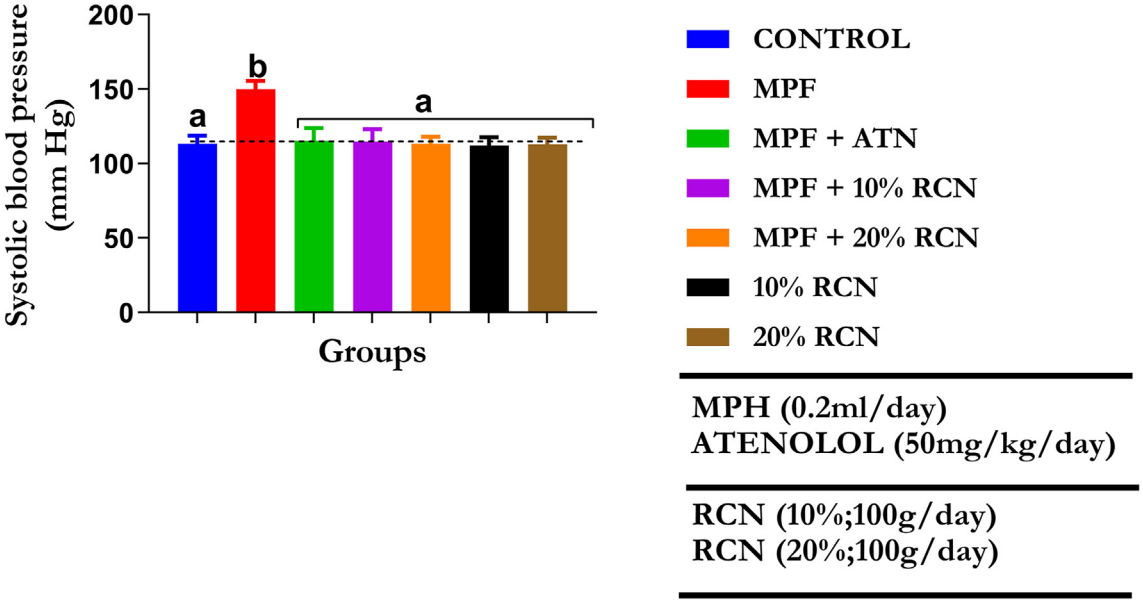

Figure 7. Effect of RCN supplementation on systolic blood pressure in rats exposed to MPH. Values are represented as mean ± SEM (n = 5). Bars with different letters are significantly different.

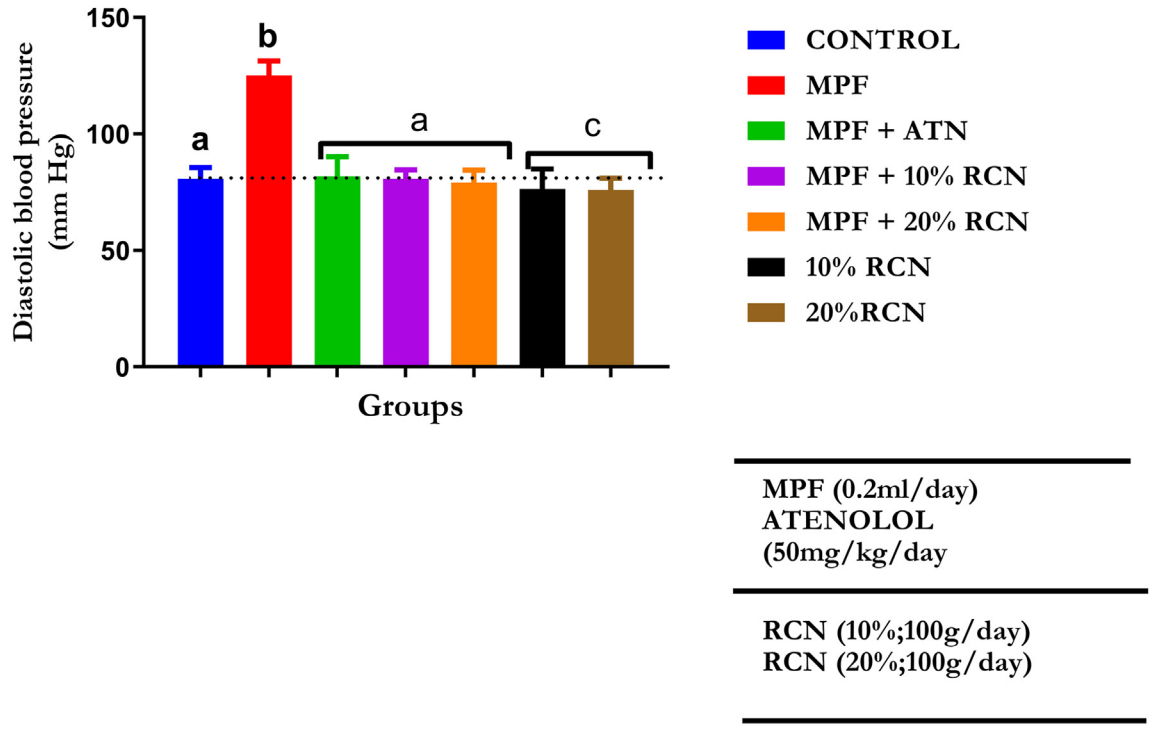

Figure 8. Effect of RCN supplementation on diastolic blood pressure in rats exposed to MPH. Values are represented as mean ± SEM (n = 5). Bars with different letters are significantly different.

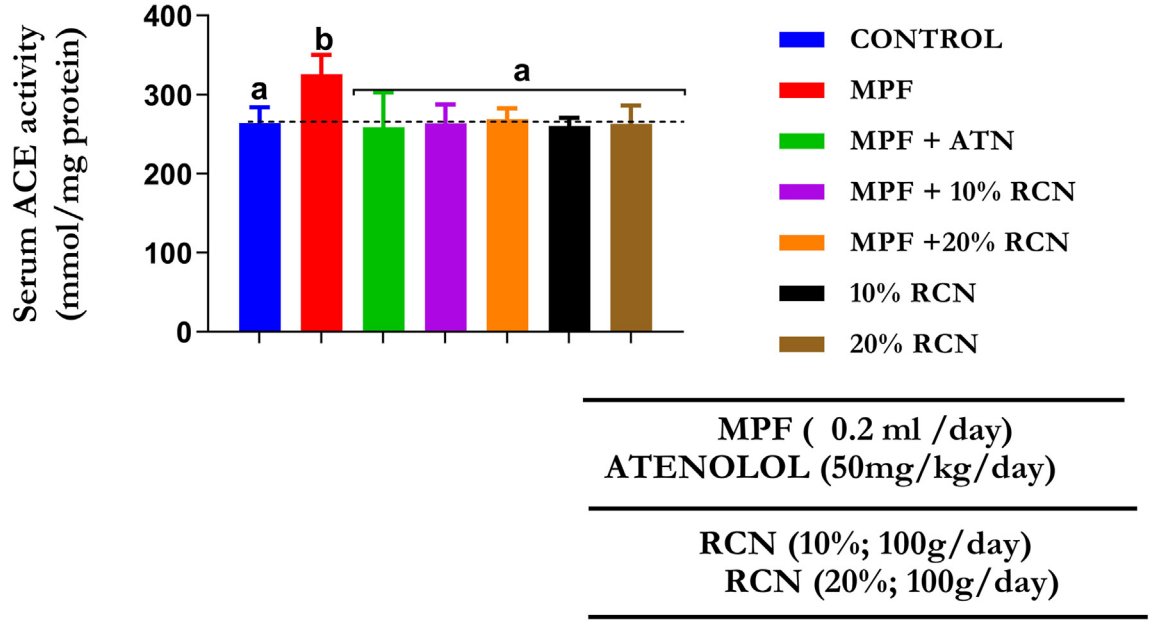

Figure 9. Effect of RCN supplementation on ACE activities in rats exposed to MPH. Values are represented as mean ± SEM (n = 5). Bars with different letters are significantly different.

agreement with other investigations [35, 36] and this may suggest that MPF can stimulate angiotensin II, a potent vasoconstrictor in the endothelial tissue. RCN supplementary diet is found to reduce ACE activities in the serum of rats in the treated groups. Nonetheless, the reduction in blood pressure could be due to the synergy of the phenolic chemicals found in RCN. In hypertensive rats, phenolic substances such quercetin, gallic acid, and rutin have been shown to reduce blood pressure [37, 38, 39].

6. Conclusions

Dietary supplementation of RCN inhibited ACE activity as well as systolic blood pressure in MPF-induced hypertensive rats. These activities could point to a mechanism of action for traditional medicine's antihypertensive advantages. Moreover, computational validation attributed the observed effect to the phenolic compounds quercetin and rutin acting in synergy or additively.

Declarations

Author contribution statement

Jacob Kehinde Akintunde: Conceived and designed the experiments; Analyzed and interpreted the data; Contributed reagents, materials, analysis tools or data; Wrote the paper.

Victoria Omoyemi Akomolafe: Conceived and designed the experiments; Performed the experiments; Analyzed and interpreted the data; Contributed reagents, materials, analysis tools or data; Wrote the paper.

Odunayo Anthonia Taiwo; Iqrar Ahmad; Harun Patel; Oluwafemi Adeleke Ojo: Performed the experiments; Analyzed and interpreted the data; Contributed reagents, materials, analysis tools or data; Wrote the paper.

Adeola Osifeso; Oluwafemi Olusegun Adefuye: Performed the experiments; Contributed reagents, materials, analysis tools or data;

Funding statement

This research did not receive any specific grant from funding agencies in the public, commercial, or not-for-profit sectors.

Data availability statement

Data will be made available on request.

Declaration of interest's statement

The authors declare no conflict of interest.

Additional information

Supplementary content related to this article has been published online at https://doi.org/10.1016/j.heliyon.2022.e12339.

References

[1] Abdullah M. Alzahrani, Peramaiyan Rajendran, Petroleum Hydrocarbon and Living Organisms, Hydrocarbon Pollution and its Effect on the Environment, Muharrem Ince and Olcay Kaplan Ince, IntechOpen, 2019.
[2] A. Fowzia, A.N.M. Fakhruddin, A review on environmental contamination of petroleum hydrocarbons and its biodegradation, Int J Environ Sci Nat Res 11 (3) (2018), 555811.
[3] P. Grandjean, P.J. Landrigan, Neurobehavioural effects of developmental toxicity, Lancet Neurol. 13 (3) (2014) 330–338.
[4] S. Babak, L. Zhen, N. Corinna, S. Bonaventura, K. Frauke, A. Mauro, G. Sibylle, G. Robert, S. Hagen, S. Norbert, M. Gernot, The tissue renin-angiotensin system and its role in the pathogenesis of major human diseases: quo vadis? Cells 10 (2021) 650.
[5] Steven D. Crowley, Nathan P. Rudemiller, Effects of the renin-angiotensin system, J. Am. Soc. Nephrol. 28 (2017) 1350–1361.
[6] A. Sala-Vila, E. Ramon, R. Emilio, New insights into the role of nutrition in CVD prevention, Curr. Cardiol. Rep. 17 (5) (2015) 583.
[7] A. Mustapha, G. Owuna, J. Ogaji, Is-haq ishaq G., idris M. Phytochemical screening and inhibitory activities of Anacardium occidentale leave extracts against some clinically important bacterial isolates, International Journal of Pharmacognosy and Phytochemical Research 7 (2) (2015) 365–369.
[8] O.A. Taiwo, O.A. Dosumu, E.O. Oni, V.O. Akomolafe, S.T. Elazab, S. Qusti, E.M. Alshammari, G.E.-S. Batiha, O.A. Ojo, 2021. Preclinical prediction of phytochemicals identified from cannabis as novel inhibitors of TEX 11, DHCR24, and CatSper 1 in fertility drug design, Inform. Med. Unlocked 26 (2021), 100747.
[9] S. Omosuli, T. Ibrahim, D. Oloye, R. Agbaje, B. Jude-Ojei, Proximate and mineral composition of roasted and defatted cashew nut (anarcadium occidentale) flour, Pakistan J. Nutr. 8 (10) (2009) 49–51.
[10] R. Pawara, I. Ahmad, S. Surana, H. Patel, Computational identification of 2,4-disubstituted amino-pyrimidines as L858R/T790M-EGFR double mutant inhibitors using pharmacophore mapping, molecular docking, binding free energy calculation, DFT study and molecular dynamic simulation, Silico Pharmacol 6 (1) (2021) 54.
[11] D. E. Shaw Research, Schrödinger Release (2021-1). Desmond Molecular Dynamics System. Maestro-Desmond interoperability tools.
[12] A. Malani, A. Makwana, J. Monapara, I. Ahmad, H. Patel, N. Desai, Synthesis, molecular docking, DFT study, and in vitro antimicrobial activity of some 4-(biphenyl-4-yl)-1,4-dihydropyridine and 4-(biphenyl-4-yl)pyridine derivatives, J. Biochem. Mol. Toxicol. (2021), e22903. Advance online publication.
[13] H. Patel, A. Ansari, R. Pawara, I. Ansari, H. Jadhav, S. Surana, Design and synthesis of novel 2,4-disubstituted aminopyrimidines: reversible non-covalent T790M EGFR inhibitors, J. Recept. Signal Transduct. Res. 38 (5-6) (2018) 393–412.
[14] H. Patel, I. Ahmad, H. Jadhav, R. Pawara, D. Lokwani, S. Surana, Investigating the Impact of Different Acrylamide (Electrophilic Warhead) on Osimertinib's Pharmacological Spectrum by Molecular Mechanic and Quantum Mechanic Approach. Combinatorial Chemistry & High Throughput Screening, 2020, 10.2174/1386207323666201204125524. Advance online publication.
[15] I. Ahmad, D. Kumar, H. Patel, Computational investigation of phytochemicals from Withania somnifera (Indian ginseng/ashwagandha) as plausible inhibitors of GluN2B-containing NMDA receptors, J. Biomol. Struct. Dyn. (2021 May 10) 1–13.
[16] R. Pawara, I. Ahmad, D. Nayak, S. Wagh, A. Wadkar, A. Ansari, S. Belamkar, S. Surana, C. Nath Kundu, C. Patil, H. Patel, Novel, selective acrylamide linked quinazolines for the treatment of double mutant EGFR-L858R/T790M Non-Small-Cell lung cancer (NSCLC), Bioorg. Chem. 115 (2021), 105234.
[17] W.L. Jorgensen, D.S. Maxwell, J. Tirado-Rives, Development and testing of the OPLS all atom force field on conformational energetics and properties of organic liquids, J. Am. Chem. Soc. 118 (45) (1996) 11225–11236.
[18] G. Kalibaeva, M. Ferrario, G. Ciccotti, Constant pressure-constant temperature molecular dynamics: a correct constrained NPT ensemble using the molecular virial, Mol. Phys. 101 (6) (2003) 765–778.
[19] G.J. Martyna, Remarks on "Constant-temperature molecular dynamics with momentum conservation, Phys Rev E Stat Phys Plasmas Fluids Relat Interdiscip Topics 50 (4) (1994) 3234–3236.
[20] R. Girase, I. Ahmad, R. Pawara, H. Patel, Optimizing cardio, hepato and phospholipidosis toxicity of the Bedaquiline by chemoinformatics and molecular modelling approach, SAR QSAR Environ. Res. (2022) 1–21. Advance online publication.
[21] Y.O. Ayipo, I. Ahmad, Y.S. Najib, S.K. Sheu, H. Patel, M.N. Mordi, Molecular modelling and structure-activity relationship of a natural derivative of o-hydroxybenzoate as a potent inhibitor of dual NSP3 and NSP12 of SARS-CoV-2: in silico study, Journal of biomolecular structure & dynamics (2022) 1–19. Advance online publication.
[22] Y. Boulaamane, I. Ahmad, H. Patel, N. Das, M.R. Britel, A. Maurady, Structural exploration of selected C6 and C7-substituted coumarin isomers as selective MAO-B inhibitors, Journal of biomolecular structure & dynamics (2022) 1–15. Advance online publication.
[23] J.K. Akintunde, T.E. Akintola, G.O. Adenuga, Z.A. Odugbemi, R.O. Adetoye, O.G. Akintunde, Naringin attenuates Bisphenol-A mediated neurotoxicity in hypertensive rats by abrogation of cerebral nucleotide depletion, oxidative damage and neuroinflammation, Neurotoxicology 81 (2020) 18–33.
[24] D.W. Cushman, H.S. Cheung, Spectrophotometric assay and properties of the angiotensin-converting enzyme of rabbit lung, Biochem. Pharmacol. 20 (7) (1971) 1637–1648.
[25] A.G. Gornall, C.J. Bardawill, M.M. David, Determination of serum proteins by means of the biuret reaction, J. Biol. Chem. 177 (2) (1949) 751–766.
[26] S. Ghosh, S. Das, I. Ahmad, H. Patel, In silico validation of anti-viral drugs obtained from marine sources as a potential target against SARS-CoV-2 Mpro, J. Indian Chem. Soc. 98 (12) (2021), 100272.
[27] R. Zrieq, I. Ahmad, M. Snoussi, E. Noumi, M. Iriti, F.D. Algahtani, H. Patel, M. Saeed, M. Tasleem, S. Sulaiman, K. Aouadi, A. Kadri, Tomatidine and patchouli alcohol as inhibitors of SARS-CoV-2 enzymes (3CLpro, PLpro and NSP15) by molecular docking and molecular dynamics simulations, Int. J. Mol. Sci. 2 (19) (2021), 10693, 22.
[28] D. Ojeda, E. Jiménez-Ferrer, A. Zamilpa, A. Herrera-Arellano, J. Tortoriello, L. Alvarez, Inhibition of angiotensin converting enzyme (ACE) activity by the anthocyanins delphinidin- and cyanidin-3-*O*-sambubiosides from *Hibiscus sabdariffa*, J. Ethnopharmacol. 127 (1) (2010) 7–10.
[29] D.E. Stevenson, R.D. Hurst, Polyphenolic phytochemicals – just antioxidants or much more? Cell. Mol. Life Sci. 64 (22) (2007) 2900–2916.
[30] C.Q. Celina, M.S. Madruga, M.M. Pintado, H.O. Gabriel, A.P. Almeida, A.D. Francileide, J.K. Bezerra, M.F. Tavares de Melo, B.V. Vanessa, B.S. Juliana Késsia, Cashew nuts (*Anacardium occidentale* L.) decrease visceral fat, yet augment glucose in dyslipidemic rats, Public Library of Science ONE 14 (12) (2019), e0225736.
[31] O.A. Ojo, A.B. Ojo, O.A. Taiwo, O.M. Oluba, 2021. Novel coronavirus (sars-cov-2) main protease: molecular docking of puerarin as a potential inhibitor, Malays. J. Biochem. Mol. Biol. (1) (2021) 108–114.
[32] S.R. Ahmad, M. Akand, Shaikh, et al., Synthesis, molecular modelling study of the methaqualone analogues as anti-convulsant agent with improved cognition activity and minimized neurotoxicity, J. Mol. Struct. 7 (25) (2022) 21820–21844.
[33] H.Y. Lee, D.Y. Cho, I. Ahmad, H.M. Patel, M.J. Kim, J.G. Jung, E.H. Jeong, M.A. Haque, K.M. Cho, Mining of a novel esterase (est3S) gene from a cow rumen metagenomic library with organosphosphorus insecticides degrading capability: catalytic insights by site directed mutations, docking, and molecular dynamic simulations, Int. J. Biol. Macromol. 190 (2021 Nov 1) 441–455.
[34] U. Acar Çevik, I. Celik, A. Işık, I. Ahmad, H. Patel, Y. Özkay, Z.A. Kaplancıklı, Design, synthesis, molecular modeling, DFT, ADME and biological evaluation studies of some new 1,3,4-oxadiazole linked benzimidazoles as anticancer agents and aromatase inhibitors, Journal of biomolecular structure & dynamics (2022) 1–15. Advance online publication.
[35] O.M. Azeez, R.E. Akhigbe, C.N. Anigbogu, Exposure to petroleum hydrocarbon: implications in lung lipid peroxidation and antioxidant defense system in rat, Toxicol. Int. 19 (3) (2012) 306–309.
[36] M.A. Oyebisi, R.A. Akhigbe, C.N. Anigbogu, Oxidative status in rat kidney exposed to petroleum hydrocarbons, J. Nat. Sci. Biol. Med. 4 (1) (2013) 149–154. International 19(3):306-309.

[37] K.S. Bhullar, G. Lassalle-Claux, M. Touaibi, H.P.V. Rupasinghe, Antihypertensive effect of caffeic acid and its analogs through dual renin-angiotensin aldosterone system inhibition, Eur. J. Pharmacol. 730 (2014) 125–132.

[38] X.F. Pang, L.H. Zhang, F. Bai, N.P. Wang, A. Shah, R. Garner, et al., Dual ACE-inhibition and angiotensin II AT1 receptor antagonism with curcumin attenuate maladaptive cardiac repair and improve ventricular systolic function after myocardial infarction in rat heart, Eur. J. Pharmacol. 746 (2015) 22–30.

[39] N. Kang, J.H. Lee, W.W. Lee, J.Y. Ko, E.A. Kim, J.S. Kim, et al., Gallic acid isolated from *Spirogyra* sp. Improves cardiovascular disease through a vasorelaxant and antihypertensive effect, Environ. Toxicol. Pharmacol. 39 (2015) 764–772.